# Multi-Contact Locomotion on Transfemoral Prostheses via Hybrid System Models and Optimization-Based Control

Huihua Zhao[1], Jonathan Horn[2], Jacob Reher[1], Victor Paredes[2] and Aaron D. Ames[3]

***Abstract*—Lower-limb prostheses provide a prime example of cyber-physical systems (CPSs) requiring the synergistic development of sensing, algorithms and controllers. With a view towards better understanding CPSs of this form, this paper presents a systematic methodology using multi-domain hybrid system models and optimization-based controllers to achieve human-like multi-contact prosthetic walking on a custom-built prosthesis: AMPRO. To achieve this goal, unimpaired human locomotion data is collected and the nominal multi-contact human gait is studied. Inspired by previous work which realized multi-contact locomotion on a bipedal robot AMBER2, a hybrid system based optimization problem utilizing the collected reference human gait as reference is utilized to formally design stable multi-contact prosthetic gaits that can be implemented on the prosthesis directly. Leveraging control methods that stabilize bipedal walking robots—control Lyapunov function based quadratic programs coupled with variable impedance control—an online optimization-based controller is formulated to realize the designed gait in both simulation and experimentally on AMPRO. Improved tracking and energy efficiency are seen when this methodology is implemented experimentally. Importantly, the resulting multi-contact prosthetic walking captures the essentials of natural human walking both kinematically and kinetically.**

***Index Terms*—transfemoral prosthesis, cyber-physical-system, hybrid system, optimization, control Lyapunov function**

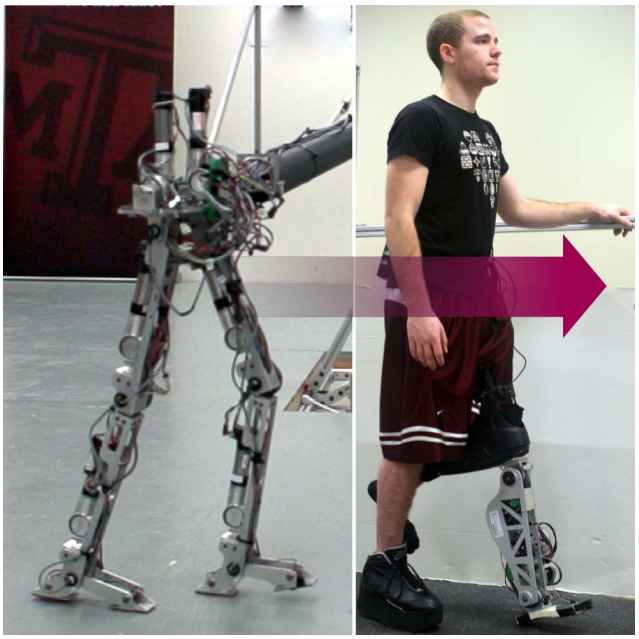

Fig. 1: Multi-contact locomotion capable bipedal robot AMBER2 (**A**dvanced **M**echanical **B**ipedal **E**xperimental **R**obotics, left) and healthy human subject with the prosthesis AMPRO (**AM**BER **Pro**sthesis) in a multi-contact posture (right).

### Note to Practitioners:

Variable impedance control, as one of the most popular prosthetic controllers, has been used widely on powered prostheses with notable success. However, due to the passivity of this controller, it requires substantial hand tuning and heuristic feedback is required to adjust the control parameters for different subjects and motion modes. The end result is extensive testing time for the users, coupled with non-optimal performance of the prostheses. Motivated by the shortcomings in the current state of the art, this work proposes a novel systematic methodology—including gait generation and optimization-based control based on a multi-domain hybrid system—to achieve prosthetic walking for a given subject. This method also aims to improve control optimality and efficiency while reducing clinical tuning.

The overarching technology utilized in this paper is the use of nominal human trajectories coupled with formal models and controllers that circumvent the need for excessive hand-tuning. In particular, rather than using a prerecorded trajectory (as is common), this work takes a different approach by using a human-inspired optimization problem to design a human-like gait for the amputee automatically. The proposed optimization framework uses the trajectory of a healthy subject as the reference and is subject to specific constraints (to ensure smooth transitions, torque and angle limitations) such that the output gait is applicable for implementation on the prosthetic devices directly. The results of the offline optimization are then utilized to synthesize an online real-time optimization-based feedback controller that allows for point-wise optimal tracking on the prosthesis, thereby improving overall efficiency. The experiment results in this work suggest that this approach is able to achieve stable human-like multi-contact prosthetic walking and also guarantees a more balanced performance compared to other traditional controllers (such as PD).

## I. INTRODUCTION

As an important application of bipedal robotics research, powered lower-limb prostheses are a prime example of cyber-physical systems (CPSs) requiring safety critical interaction between a human and prosthetic device. During the course of a

*NSF CAREER Award CNS-0953823 and Texas Emerging Technology Fund 11062-013. This research has approval from the Institutional Review Board with IRB2014-0382F for testing with human subjects.

[1]H. Zhao and J. Reher are with the School of Mechanical Engineering, Georgia Institute of Technology, Atlanta, GA, USA. {huihua, jpreher}@gatech.edu

[2]J. Horn and V. Paredes are with the department of Mechanical Engineering, Texas A&M University, College Station, TX, USA. {j.horn, vcparedesc}@tamu.edu

[3]Prof. A. D. Ames is with the School of Mechanical Engineering and the School of Electrical and Computer Engineering, Georgia Institute of Technology, Atlanta, GA, USA. ames@gatech.edu

step, the human leg and the prosthetic device interchange roles between weight bearing (stance phase) and swing forward (swing phase) phases. Moreover, interactions between the human, device and environment change in a multi-contact fashion, e.g., with the heel or toe leaving and impacting walking surface [3], [33]. With this behavior in mind, a synergistic development of sensing, algorithms and controllers for the correct and safe collaboration between the human and the device are required for natural and efficient robotic-assisted locomotion.

The multi-domain, or multi-contact nature of the human gait results in walking which is both fluid and efficient [21]. Using the foot push off during the single support phase, a human can lift the swing leg higher, and thus achieve greater foot clearance without bending the swing knee significantly. By having the body pivoting over the the stance toe, much less energy is required for a human to move forward through the utilization of their forward rotational momentum. Researchers also found that the prosthetic foot push off is negatively correlated with leading intact limb loading impulse, which may help reduce knee osteoarthritis in lower extremity amputees [25]. While exhibiting these behaviors is seemingly effortless for an unimpaired human, it is quite challenging to incorporate these advantages into bipedal robots or prostheses locomotion.

Multi-contact locomotion, which utilizes complex foot behaviors, has been studied actively in the robotics and control field throughout the recent decade. In this setting, methods utilizing the popular Zero Moment Point, including gait pattern generation and gait planning methods, are adopted to design the foot trajectory specifically for multi-contact foot behavior in [10], [15], [19] with foot roll only during the double support phase. Simulated robotic walking with significant foot push can be found in [12], [34], in which the authors show that the walking gait with foot push off helps reduce torque and achieve faster walking speeds. In contrast to these approaches, previous work by the authors [23], [41] started with a hybrid system model of human locomotion [8], [13], and proposed a novel multi-domain optimization problem which embeds this multi-contact feature into gait design to generate human-like locomotion in a manner which is both formally guaranteed and physically realizable. This was combined with a trajectory reconstruction method [5], with the end result being successful experimental realization of stable human-like multi-contact locomotion on a 7-link 2D bipedal robot AMBER2 seen in Fig. 1 (see video at [1]).

The primary goal of this paper is to extend the framework used to achieve multi-contact robotic walking [41], as motivated by previous work by the authors in translating simpler locomotion behaviors to prostheses [43]. More specifically, this work will utilize a prosthetic gait that is generated based on the hybrid system model of multi-domain locomotion and an optimization-based controller that stabilizes the robotic walking. The main contributions of this paper are three-fold: (1) proposed a hybrid system model of multi-contact prosthesis locomotion along with a corresponding hybrid zero dynamics (HZD) based optimization problem that yields stable prosthesis walking gaits, (2) a real-time nonlinear optimization-based control methodology for generating and realizing multi-contact prosthesis walking gait on the custom-built prosthesis AMPRO; (3) illustrated the method for experimental implementation with the detailed analysis of the resulting multi-contact prosthetic walking. The results presented in this paper shows a) a smoother gait with natural and human-like joint movement; b) more symmetric walking with close prosthetic stance and human-stance duration and c) more comfortable user experience with foot push off when compared to flat-foot walking. Importantly, this substantially differentiates this paper from a conference version that appeared in the International Conference of Decision and Control 2015 [39]; the conference version only included the initial results on multi-contact locomotion without the detailed framework and in depth experimental evaluation. This paper, therefore, gives substantially more context and supporting experimental evidence that provides the formal framework and quantifiable metrics of improved performance. These contributions are achieved through a two-step process.

The first step is to generate a multi-contact prosthetic gait using a multi-domain hybrid system model. Based upon the fact that humans share a similar gait pattern during locomotion [14], [32], a low-cost motion capture system is used to collect reference human locomotion data from an unimpaired subject. With the collected data as a reference, a multi-domain optimization problem—subject to constraints determined by the interface between *virtual constraints* and the hybrid model—is proposed as a means to generate a customized stable multi-contact prosthetic gait. The result is an automatically generated prosthetic gait which is both theoretically sound and directly implementable on the prosthetic device, thereby essentially eliminating the necessity of hand tuning the controller.

Utlizing control methods that stabilize bipedal walking robots, in particular control Lyapunov functions [7], the second step is to formulate a quadratic program based controller that achieves rapidly exponential convergence of virtual constraints subject to actuator bounds. When this approach is synthesized with impedance control as a feed-forward term, the result is a model independent quadratic program (MIQP) based controller that is able to achieve better tracking and improved energy efficiency on prostheses. This controller was first verified in simulation and tested on a human-like bipedal robot platform: AMBER [40]. The systematic methodology was then successfully translated to a custom built prosthesis AMPRO for achieving both flat-foot level ground walking [43] and stair ascent [44], showing improvements on both tracking and energy efficiency compared to other controllers such as PD. With this framework in hand, the proposed real-time optimization-based controller will be utilized to realize multi-contact prosthetic walking on AMPRO.

The paper is structured as follows. The multi-contact nature of human locomotion will be revisited in Section II. The automatic multi-contact gait generation process, utilizing human-inspired optimization, is discussed in Section III. Section IV reviews the real-time optimization-based controller briefly and discusses the results of simulated multi-contact prosthetic walking. The experimental realization of both the multi-contact gait and the proposed controller is illustrated in Section V.

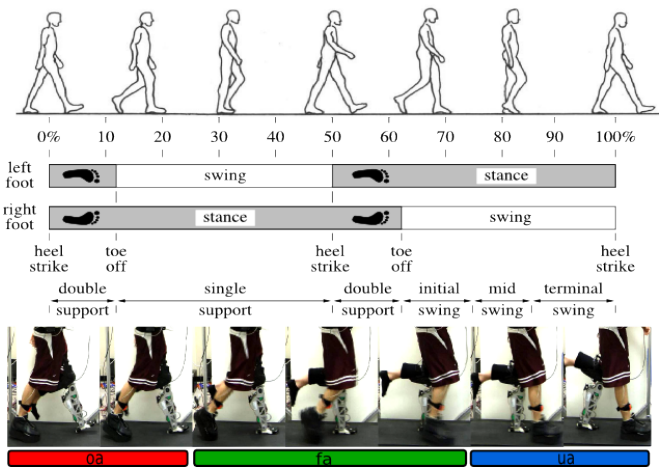


Fig. 2: Multi-contact locomotion diagram of a typical human gait cycle [3] (top) and multi-contact domain break of the AMPRO prosthetic walking (bottom).

## II. Multi-Domain Human Locomotion

This section begins with reviewing the multi-domain behavior embedded in human locomotion [3], [8], [41]. A motion capture system with inertial measurement units (IMUs) is developed to obtain the nominal human locomotion data for an unimpaired subject; this will be utilized as a reference for the purpose of prosthetic gait design. The collected data for the subject is compared with averaged human locomotion trajectories [37] in Fig. 3, where reasonable agreement is seen.

### A. Multi-Domain Human Locomotion

The nominal human walking pattern is of obvious importance when attempting to reproduce natural looking behaviors on robots or prostheses. At the highest level, a human walking gait normally is divided into two phases consisting of a single support phase in which only one foot is in contact with the ground and a double support phase in which both feet are in contact with the walking surface as depicted in Fig. 2. Sub-phases are usually extracted from each phase to describe human locomotion more explicitly. The work in this paper breaks each step into three distinct sub-phases based on the points of the feet that are in contact with the ground.

Utilizing the acceleration-based domain breakdown method discussed in [42], three domains (i.e., sub-phases) of a single step are considered as motivated by the multi-contact walking achieved on the bipedal robot AMBER2 [41]. Based on the actuation type and contact points, we denote the three domains as over-actuated domain, *oa* (with the stance heel and swing toe in contact with the ground), fully-actuated domain, *fa* (with the stance heel and toe in contact with the ground) and under-actuated-domain, *ua* (with only stance toe in the ground) as shown in Fig. 2. The switching between domains is triggered by the changes of contact points of the feet. A detailed hybrid system model based upon the multi-contact model of human walking will be developed in Section III. First, the method for collection human data will be discussed.

### B. Invariant Human Trajectory Reference

Reproducing the multi-contact behavior of human gaits in prosthetic walking is important for symmetric, natural and efficient walking on an amputee. One obvious problem encountered when designing such a gait is the lack of a nominal gait reference specific to the amputee. Human gait researchers and biomechanists have found that humans share a common pattern of joint trajectories during locomotion [37]. Therefore, a feasible approach is to use the nominal trajectories obtained from healthy subjects as the initial test gait for the amputee. While this is a common practice for prosthesis researchers and clinical physicians [14], [32], this approach requires hand tuning and heuristic experience. This motivates the proposed approach of formulating an optimization problem to formally design a gait for the amputee automatically. Building upon previous work, we propose a method to utilize the reference gait from an unimpaired subject that has similar anthropomorphic parameters (w.r.t. limb length) to the amputee as the reference for automatic prosthetic gait design.

### C. Motion Capture with IMU

In order to obtain a gait from the reference subject, a low-cost motion capture system is developed for user locomotion trajectory collection. In particular, a model based Extended Kalman Filter (EKF) utilizing the filter presented by [31] is used to obtain accurate joint angle information about the human subject. During the experiment, the subject was asked to walk along a straight line with a self-selected cadence for several steps. The joint angles and velocities are estimated and collected from the EKF algorithm, and then several steps are averaged to yield their unique trajectories for optimization. These captured trajectories by the IMUs are compared with the nominal human trajectories obtained from Winter's data [37]. The results in Fig. 3 indicate that the IMU system is able to capture the human locomotion trajectory quantitatively.

Note that, we did not perform a multi-subject validation of this estimation algorithm as it is not central to the topic of this paper. Since the authors in [31] validated the 3D filtering method, we are assuming in this work that a planar projection of the method will capture the information we seek accurately. Specifically, the captured data of our single user is not statistically relevant for the purposes of claiming a validation of the method. Instead, the aim of Fig. 3 is to show that the saggital plane trajectories are qualitatively human-like through a comparison of the data to a widely used dataset [37]; therefore, the captured data can be used as a reasonable seed for the prosthetic gait design.

## III. Multi-Contact Prosthetic Gait Generation

One of the main contributions of this work is the translation of the methodology previously utilized for designing multi-contact walking gaits for the bipedal robot AMBER2 to design walking gaits for prostheses in an automatic fashion. In particular, a multi-domain bipedal hybrid system with anthropomorphic parameters is considered to be a "human" model for the purpose of prosthetic gait design. Based on this model and the reference human locomotion data obtained

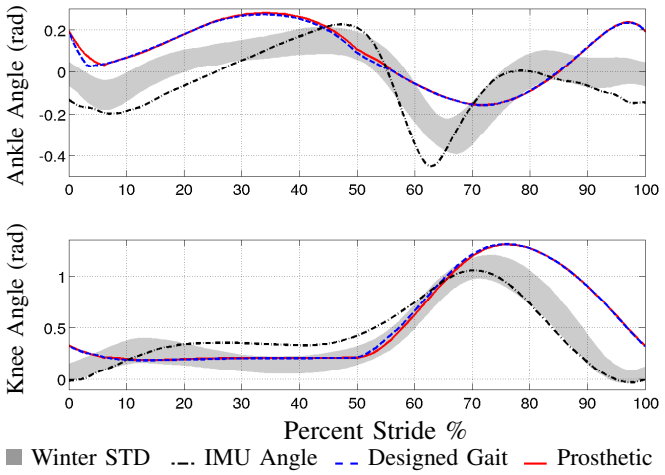


Fig. 3: Joint angles for human subject collected with IMUs, the designed prosthetic gait and the simulated prosthetic walking joint trajectories compared to Winter [37]. The trajectories (i.e., Winter data) are used as a comparison to show that the subject is walking with qualitatively human-like trajectories for use as a seed in the trajectory optimization.

with the IMUs, a hybrid system model based human-inspired optimization [23] is implemented to generate a human-like prosthetic gait that (a) yields theoretically provable stability, (b) captures the essential multi-contact behaviors of healthy human walking, (c) suits the specific test subject wearing the prosthetic device and (d) can be implemented on the prosthetic device directly.

### A. Multi-Domain Hybrid Model

A hybrid system model with both continuous dynamics and discrete dynamics is developed to properly represent the changing dynamics of the device throughout the various foot contact events (lifting and striking of the heel and toe) in a gait cycle. This hybrid model can be formally written as the following tuple [8], [13]:

$$\mathscr{HC} = (\Gamma, D, U, S, \Delta, FG), \tag{1}$$

where

- $\Gamma = (V, E)$ is a *directed cycle*, with vertices $V = \{oa, fa, ua\}$; and edges $E = \{e_1 = \{oa \to fa\}, e_2 = \{fa \to ua\}, e_3 = \{ua \to oa\}\}$,
- $D = \{D_{oa}, D_{fa}, D_{ua}\}$, set of *domains of admissibility*,
- $U = \{U_{oa}, U_{fa}, U_{ua}\}$, set of *admissible controls*,
- $S = \{S_{oa\to fa}, S_{fa\to ua}, S_{ua\to oa}\}$, set of *guards*,
- $\Delta = \{\Delta_{oa\to fa}, \Delta_{fa\to ua}, \Delta_{ua\to oa}\}$, set of *reset maps*,
- $FG = \{(f_v, g_v)\}_{v\in V}$ with $(f_v, g_v)$ a *control system* on $D_v$, i.e., $\dot{x} = f_v(x) + g_v(x)u_v$ for $x \in D_v$ and $u_v \in U$.

The detailed mathematical construction of this hybrid system representation is not a major focus in this work. For readers who are interested about the explicit derivation can be referred to [23], [41].

The configuration space of the robot $Q$ is characterized by the generalized coordinates $\theta = \{p_x, p_z, \psi_0, \theta_b\}$, where the extended coordinates $\{p_x, p_z, \psi_0\}$ represent the position and rotation angle of the body fixed frame $R_b$ with respect to a fixed inertial frame $R_0$; and $\theta_b = \{\theta_{sa}, \theta_{sk}, \theta_{sh}, \theta_{nsh}, \theta_{nsk}, \theta_{nsa}\}$ denotes the body coordinates of the model shown in Fig. 4. The dynamics on each domain will be obtained from general "unpinned" model through the use of holonomic constraints [27], [35]. Particularly, the equations of motion for the continuous dynamics are obtained using the Euler-Lagrange formula and the holonomic constraints:

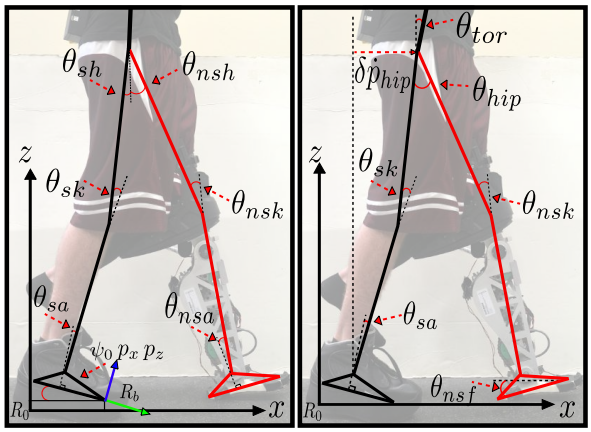


Fig. 4: Coordinates (left) and outputs configuration (right) of the multi-contact robotic model.

$$\begin{aligned} &M(\theta)\ddot{\theta} + H(\theta, \dot{\theta}) = B_v(\theta)u + J_v(\theta)^T F_v(\theta, \dot{\theta}, u), \\ &J_v(\theta)\ddot{\theta} + \dot{J}_v(\theta)\dot{\theta} = \mathbf{0}, \end{aligned} \tag{2}$$

where $M(\theta) \in \mathbb{R}^{9\times 9}$ is the inertial matrix. $H(\theta, \dot{\theta}) = C(\theta, \dot{\theta})\dot{\theta} + G(\theta) \in \mathbb{R}^{9\times 1}$ contains the terms resulting from the Coriolis effect, centrifugal forces and the gravity vector. $B_v(\theta)$ denotes the torque distribution matrix of domain $v$ and $u \in U$ is the input torque vector. $F_v(\theta, \dot{\theta}, u)$ is a vector containing a contact wrench for each point on the robot in contact with the walking surface and $J_v(\theta)$ is the corresponding Jacobian matrix of the holonomic constraints, i.e., the contact points of a particular domain. To be more specific, the elements of the Jacobian matrix are the first-order partial derivatives of the generalized position vector (including both the translational position and the planar rotation) of the contact points.

With the notation $x = (\theta; \dot{\theta})$, the affine control system $\dot{x} = f_v(x) + g_v(x)u$ for each domain $D_v$ with $v \in V$ can be obtained by reformulating (2) [30]. The discrete behavior, $\Delta_e$, of impacts is modeled with the assumption of perfectly plastic impacts, i.e., there is no deformation, slippage or bounce during the impacts. This is a common practice in robotic modeling literature; more details can be found in [20], [35].

### B. Human-Inspired Outputs

Given the complexity of human locomotion (utilizing 57 muscles during the locomotion [21]), we take the perspective of viewing this system as a "black box." The goal of achieving human-like walking (i.e., obtaining a human-like gait) then becomes to drive the actual robot outputs $y^a(\theta)$ to the desired

human outputs $y^d(t,\alpha)$ that are represented by the *extended canonical walking function* (ECWF):

$$y^d(t,\alpha) = e^{-\alpha_4 t}(\alpha_1\cos(\alpha_2 t)+\alpha_3\sin(\alpha_2 t))+... \\ \alpha_5\cos(\alpha_6 t)+\kappa(\alpha)\sin(\alpha_6 t)+\alpha_7, \quad (3)$$

with $\kappa(\alpha) = (2\alpha_4\alpha_5\alpha_6/((\alpha_2)^2+(\alpha_4)^2+(\alpha_6)^2))$. For the multi-domain 7-link bipedal robot model, a total of 7 actual outputs are of interest, which can be further separated into two groups. The first group is the velocity-based relative degree one output $y_1^a(\theta,\dot\theta)\in\mathbb{R}$, i.e., the linearized forward hip velocity $\delta\dot p_{hip}(\theta)$. The second group is the relative degree two outputs $y_2^a(\theta)\in\mathbb{R}^6$, which include two knee angles $\theta_{sk}$, $\theta_{nsk}$, stance ankle angle $\theta_{sa}$, torso angle $\theta_{tor}$, hip angle $\theta_{hip}$ and non-stance foot angle $\theta_{nsf}$. The detailed convention of these outputs is shown in Fig. 4.

Additionally, from analysis of multi-contact human locomotion data, the linearized forward hip position, $\delta p_{hip}(\theta)$, was discovered to increase linearly, i.e., the hip velocity is approximately constant through the progress of a step cycle [22]. This motivates the following phase variable:

$$\rho(\theta) = (\delta p_{hip}(\theta) - \delta p_{hip}^+)/v_{hip}, \quad (4)$$

aiming to remove the dependency of time [5], [35]. $\delta p_{hip}^+(\theta)$ is the initial hip position at the beginning of a step, which is decided through the optimization problem that will be discussed in the following sections.

Therefore, the virtual constraints can be represented as: [5]

$$y(\theta,\dot\theta,\alpha)=\begin{bmatrix} y_1(\theta,\dot\theta,\alpha)\\ y_2(\theta,\alpha)\end{bmatrix}=\begin{bmatrix} y_1^a(\theta,\dot\theta)-v_{hip}\\ y_2^a(\theta)-y_2^d(\rho(\theta),\alpha)\end{bmatrix}, \quad (5)$$

where $y_1(\theta,\dot\theta,\alpha)\in\mathbb{R}$ is the relative degree one virtual constraint, which is the difference between the actual hip velocity $y_1^a(\theta,\dot\theta)$ and the desired hip velocity $v_{hip}$[1]. The vector $y_2(\theta,\alpha)\in\mathbb{R}^6$ contains the relative degree two human-inspired outputs which are the differences between the actual outputs $y_2^a(\theta)$ and desired outputs $y_2^d(\rho(\theta),\alpha)$. Note that the parameter set $\alpha$ is the grouped parameters of all the outputs for a complete step cycle [41]. Based on the actuation type in each domain $D_v$ with $v\in V$, the corresponding components $\alpha_v$ of $\alpha$ will be utilized to characterize the human-inspired outputs via (3). For example, for the fully-actuated domain *fa*, one relative degree one output and five relative degree two outputs are considered [41]. The parameters will be kept the same for all the domains for a specific output, i.e., only one parameter set $\alpha$ is used to characterize an entire step.

**Partial Hybrid Zero Dynamics (PHZD).** A feedback linearization controller (as in [35], [36]) can be utilized to drive both $y_1\to 0$ and $y_2\to 0$ exponentially for the continuous dynamics. However, the robot will be "thrown off" the designed trajectory when impacts occur. This motivates the introduction of the PHZD constraints aiming to yield a parameter set $\alpha$ that ensures the tracking of relative degree two outputs remain invariant through impacts [**?**]. In particular, with the *partial zero dynamics* surface defined:

$$\mathbf{PZ}_\alpha = \{(\theta,\dot\theta)\in TQ : y_2(\theta,\alpha)=\mathbf{0}, L_f y_2(\theta,\alpha)=\mathbf{0}\}, \quad (6)$$

[1]The desired relative degree one output $v_{hip}$ can be viewed as a special case of the ECWF with $\alpha_{1,...,6}=0$ and $\alpha_7=v_{hip}$

the general PHZD constraints can be stated as:

$$\Delta(S\cap\mathbf{PZ}_\alpha)\subseteq\mathbf{PZ}_\alpha, \quad \text{(PHZD)}$$

which are required to be valid through all the three discrete transitions as illustrated in (1). Particularly, the three sets of PHZD constraints can be stated as:

$$\Delta_{oa\to fa}(S_{oa\to fa}\cap\mathbf{PZ}_{\alpha_{oa}})\subseteq\mathbf{PZ}_{\alpha_{fa}}, \quad \text{(PHZD1)}$$
$$\Delta_{fa\to ua}(S_{fa\to ua}\cap\mathbf{PZ}_{\alpha_{fa}})\subseteq\mathbf{PZ}_{\alpha_{ua}}, \quad \text{(PHZD2)}$$
$$\Delta_{ua\to oa}(S_{ua\to oa}\cap\mathbf{PZ}_{\alpha_{ua}})\subseteq\mathbf{PZ}_{\alpha_{oa}}. \quad \text{(PHZD3)}$$

These three PHZD constraints ensure that the virtual constraints of each domain remain invariant through all the discrete transitions, therefore, guarantee the smoothness of the designed gait obtained from the optimization problem. The detailed mathematical construction of these constraints requires the explicit explanation of techniques such as the reduced order hybrid zero dynamics, inverse kinematics and PHZD reconstructions, which are not the focus of this work and omitted here. The details can be referred to [23], [41].

### C. Multi-Contact Prosthetic Gait Design

Enforcing the PHZD constraints discussed above, a multi-domain optimization is utilized to design stable human-like prosthetic gaits automatically. For the cyber-physical system of a lower-limb prosthesis interacting with humans in a safety critical fashion, physical constraints incorporating (a) hardware limits (torque limits and joint movement range), (b) safety concern (foot clearance and impact velocity) and (c) user comfort (user preferred trajectory profile) are explicitly considered during the gait design optimization [43]. These specifications yield the optimization problem subject to both the PHZD constraints and the physical constraints as follows:

$$\alpha^* = \underset{\alpha\in\mathbb{R}^{43}}{\operatorname{argmin}}\ \text{Cost}_{\text{HD}}(\alpha) \quad (7)$$
$$\text{s.t} \quad \text{(PHZD1)}-\text{(PHZD3)},$$
$$\text{Physical Constraints},$$

where the cost function is the least-square-fit error between the unimpaired human reference data and the ECWF representations in (3). The end result of this optimization problem is the outputs parameter set $\alpha$ that renders an optimal (w.r.t. torque, foot clearance, joint position and velocity) and provably stable subject-like multi-contact prosthetic gait, which at the same time can be implemented directly on the prosthetic device. The desired joint angles and angular velocities for the prosthetic device can be obtained through the inverse projection from the PHZD surface by only knowing the actual forward hip position $\delta p_{hip}$ and the corresponding hip velocity $\delta\dot p_{hip}$. In particular, the hip position $\delta p_{hip}$ is used for the desired position calculation based on (3) and (4) and the $\delta\dot p_{hip}$ will be used for desired velocity calculation based on the derivation of (3) and (4), more details of which can be referred to [5], [41]. With this PHZD reconstruction methodology, the designed trajectories of both the ankle and knee joint, shown in Fig. 3, are obtained and compared with the nominal human locomotion data obtained from Winter [37]. Both the knee and

ankle angle are shown to have a similar pattern as the nominal locomotion.

**Remark.** Utilizing the gait of an unimpaired subject as reference, this optimization problem is subject to both the PHZD and physical constraints such that the generated gait is smooth, user-friendly and applicable for direct implementation on the prosthetic device. While there is no clear evidence showing that a particular gait is more comfortable or performant, the goal of the proposed methodology is that with the automation of the gait generation, hand tuning can potentially be reduced and done in a more high-level manner. For example, for the experimental walking trajectories used in this work, the initial gait was designed with more stance knee movement, i.e., the stance knee angle was more human-like with bigger knee bent. However, the test subject prefers less stance knee movement, which was reported to feel more comfortable and safer (large stance knee movement may increase the possibility of buckling during stance phase for some extreme situations). Therefore, this preference can be easily added into the optimization, the end result of which is the stance knee angle being more flat compared to the nominal human trajectory (see Fig. 3).

## IV. PROSTHETIC CONTROLLER DESIGN

This section begins with the brief introduction of the variable impedance controller commonly used in the control of prostheses [11], [18], [32]. Then, the novel real-time optimization-based prostheses controller, proposed in [40] and validated in [43] is revisited. Finally, the proposed controller is implemented to achieve multi-contact prosthetic walking with the designed trajectory in simulation at the end of this section.

### A. Impedance Control for Prosthesis

As one of the most common approaches for prosthetic control [11], [17], [18], [32], variable impedance control assumes that human gait is cyclical and the torque at each joint can be represented in a piecewise fashion by a series of passive impedance functions of the form:

$$u^{imp} = k(\theta - q^e) + b\dot{\theta}, \tag{8}$$

with $k$, $q^e$ and $b$ representing the impedance parameters for stiffness, equilibrium angle and damping, respectively, which are constant for a specific phase. Based upon previous work [4], analysis of multi-contact locomotion data obtained from human models shows that one gait cycle can be divided into four sub-phases based on the profile of prosthesis joint angles. It is important to note that the impedance sub-phases considered here are for the implementation of impedance control only, as opposed to the domains considered in the gait design process. The explicit criterion of the phase separation (which is based on the joint angles or angular velocities) is bypassed here but can be found in [4], [38].

### B. MIQP+Impedance Control

In previous work [43], the authors proposed a novel prosthetic controller which combines the *rapidly exponentially stabilizing control Lyapunov functions* (RES-CLFs) based quadratic program control [7] with impedance control in an effort to achieve better tracking and improved energy efficiency on prostheses. In particular, we consider the simplest form of a trajectory tracking problem with $\ddot{\eta} = u$, which can be converted to a linear form as follows:

$$\dot{\eta} = \underbrace{\begin{bmatrix} 0_{2\times2} & I_{2\times2} \\ 0_{2\times2} & 0_{2\times2} \end{bmatrix}}_{F} \eta + \underbrace{\begin{bmatrix} 0_{2\times2} \\ I_{2\times2} \end{bmatrix}}_{G} u, \tag{9}$$

where $\eta = (y_p; \dot{y}_p) \in \mathbb{R}^{4\times1}$ with $y_p = (y_p^{ankle}, y_p^{knee})^T$ the virtual constraints for the prosthetic ankle joint $y_p^{ankle}$ and knee joint $y_p^{knee}$, respectively, and $u \in \mathbb{R}^{2\times1}$ is the direct control input. Here we only focus on the control of the two prosthetic joints. The whole body dynamics can also be written in this linear form after applying a state-based feedback linearization controller by defining $\eta = (y; \dot{y})$ [5]. Leveraging the Continuous Algebraic Riccati Equation (CARE) with solution $P = P^T > 0$, allows for the construction of a RES-CLF [7] given as:

$$V_\varepsilon(\eta) = \eta^T \begin{bmatrix} \frac{1}{\varepsilon} I & 0 \\ 0 & I \end{bmatrix} P \begin{bmatrix} \frac{1}{\varepsilon} I & 0 \\ 0 & I \end{bmatrix} \eta := \eta^T P_\varepsilon \eta, \tag{10}$$

with the convergence rate $\varepsilon > 0$. In order to exponentially stabilize the system, we want to find $u$ such that, for a chosen $\gamma > 0$ [7], we have:

$$L_F V_\varepsilon(\eta) + L_G V_\varepsilon(\eta) u \leq -\frac{\gamma}{\varepsilon} V_\varepsilon(\eta), \tag{11}$$

where $L_F V_\varepsilon(\eta)$ and $L_G V_\varepsilon(\eta)$ are the corresponding Lie derivatives of the Lyapunov function (10) relative to (9). Particularly, an optimal (point-wise) $u$ could be found by turning this condition into a quadratic problem (QP) while enforcing a relaxation term $\delta > 0$ [7] to ensure that hardware constraints (related to maximum torque constraints $u_{MAX}^{qp}$ and $u_{MAX}$) take priority over control objectives. More importantly, we add the variable impedance term $u^{imp}$ into this construction for the total hardware torque bounds, which yields the following model independent quadratic program plus impedance control (MIQP+Impedance):

$$\begin{aligned}
\underset{(\delta, u^{qp}) \in \mathbb{R}^{2+1}}{\operatorname{argmin}} \quad & p\delta^2 + u^{qpT} u^{qp} && (12)\\
\text{s.t} \quad & L_F V_\varepsilon(\eta) + \frac{\gamma}{\varepsilon} V_\varepsilon(\eta) + L_G V_\varepsilon(\eta) u^{qp} \leq \delta, && \text{(CLF)}\\
& u^{qp} \leq u_{MAX}^{qp}, && \text{(Max QP Torque)}\\
& -u^{qp} \leq u_{MAX}^{qp}, && \text{(Min QP Torque)}\\
& u^{qp} \leq u_{MAX} - u^{imp}, && \text{(Max Input Torque)}\\
& -u^{qp} \leq u_{MAX} + u^{imp}. && \text{(Min Input Torque)}
\end{aligned}$$

This QP problem yields an optimization-based controller that regulates the error of the output dynamics in a rapidly exponentially stable fashion. Simultaneously, by adding impedance control as a feed-forward term into the input torque, the model independent dynamic system (9) gathers some information about the system that it is controlling. By setting the QP torque bounds $u_{MAX}^{qp}$, we can limit problems of overshoot. We also set the total input torque bounds for the QP problem such that the final input torque will satisfy the hardware torque bounds $u_{MAX}$, which is critical for practical implementation.

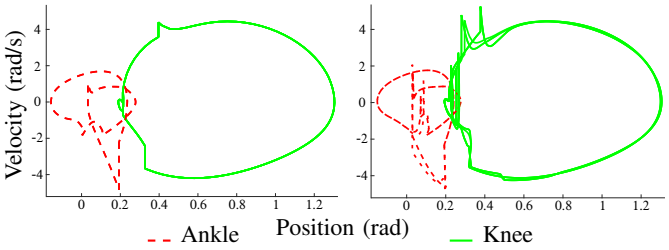


(a) Unimpaired Walking (b) Prosthetic Walking

Fig. 5: Phase portraits of the prosthesis joints of the simulated unimpaired walking and prosthetic walking.

This nonlinear optimization-based controller was first verified on a custom-built prosthetic device: AMPRO for flat-foot level ground walking with improved performance of both tracking (23% improvement) and energy efficiency (25% reduction) when compared to other existing controllers (such as PD) [43]. The main contribution of this work will extend the aforementioned controller to achieve more dynamic and human-like multi-contact level ground walking. Both the resulting multi-contact gait trajectories and torque profiles will be compared with the flat-foot prosthetic walking, showing the improved prosthetic walking in the aspects of both the user experience and natural human motions.

### C. Simulation Results

Before implementing the controller on the prosthesis, the control architecture is first verified in simulation. In particular, two simulation scenarios are considered and compared. For the first simulation, the whole bipedal robot model is controlled by the original model-based human-inspired feedback controller for perfect tracking [5], which we consider as "unimpaired" human walking. For the second simulation, the biped model is assumed to "wear" a prosthetic device which will be controlled by the decentralized (i.e., independent of the control of the residual limbs) MIQP+Impedance controller. We consider this case as the "prosthetic" walking. To be more explicit, the right leg will be assumed to be the prosthetic device (including the actuation of both the ankle and knee joints of the "prosthesis"), and the residual limbs will be controlled with the human-inspired controller with the purpose to mimic the function of the healthy human side.

The limit cycles of both the healthy human walking and the prosthetic walking are shown in Fig. 5. By looking at the shape of the two plots, we can see that the model independent optimization-based controller achieves similar walking trajectory as the model-based feedback linearization controller (i.e., the human-inspired controller [5]). It is also clear to see that the phase portrait of the proposed decentralized nonlinear controller is less smooth (i.e., not impact invariance) than the one with the human-inspired controller. While the smoothness is trivial for a centralized state-based feedback controller, this invariance is hardly possible for the decentralized prosthetic controller which lacks model information. However, due to the embedded feature of rapidly exponential convergence of the proposed controller, one can note that the phase portraits converge back (instead of blowing up) to the normal trajectory

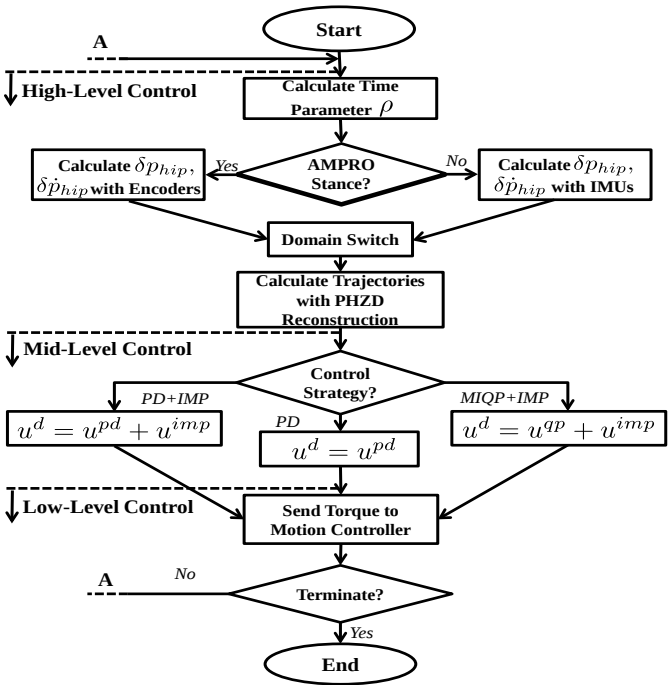


Fig. 6: Flow chart of the pseudo-code.

quickly after the impact. Similar discussion can also be found in [40].

The stability of both the multi-contact gaits was numerically validated through the Poincaré map, which is a general mathematical tool for determining the existence and stability properties of periodic orbits for hybrid dynamical systems with impulses [6], [26], [29]. In particular, with the unit of the maximum eigenvalue smaller than one, it indicates the exponential stability of the corresponding nonlinear hybrid system. With numerical approximation, the magnitude of the maximum eigenvalue was found to be $5.5e^{-8}$ using human-inspired control and $5.5e^{-4}$ using MIQP+Impedance control. The resulting joint trajectories of the simulated prosthetic walking are depicted in Fig. 3, showing that the proposed real-time optimal controller can replicate the human trajectory with remarkable similarity. Note that the pure impedance controller also has been tested in simulation. However, due to complexity of multi-contact locomotion (multiple impacts and switching between different actuation types of domains), the impedance controller can not provide stable multi-contact walking in simulation.

## V. EXPERIMENTAL REALIZATION

With the multi-contact gait generated in Sec. II and the controller introduced in Sec. IV, we now are ready to realize the main contribution of this paper experimentally on the custom-built prosthesis AMPRO to achieve dynamic multi-contact prosthetic walking. The resulting walking using the real-time optimization-based controller will be compared with several other control approaches. The proposed controller demonstrates an improved performance.

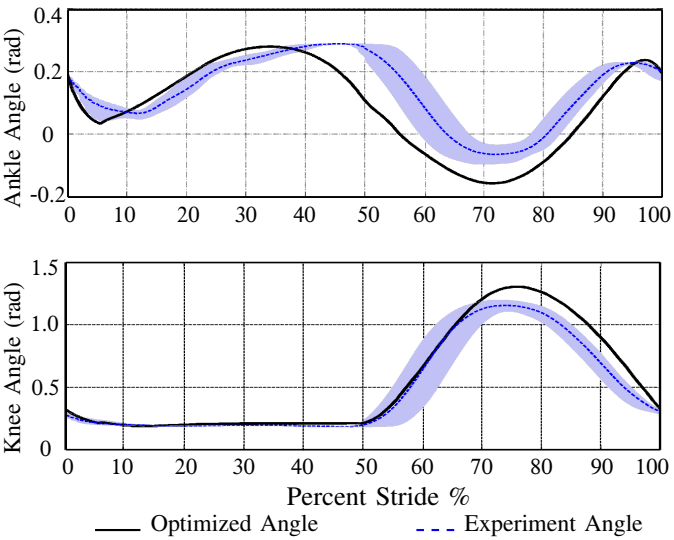


Fig. 7: Averaged experimental joint angles compared with the designed joint angles obtained from optimization. Grey area is the standard deviation of the experiment results over 10 steps.

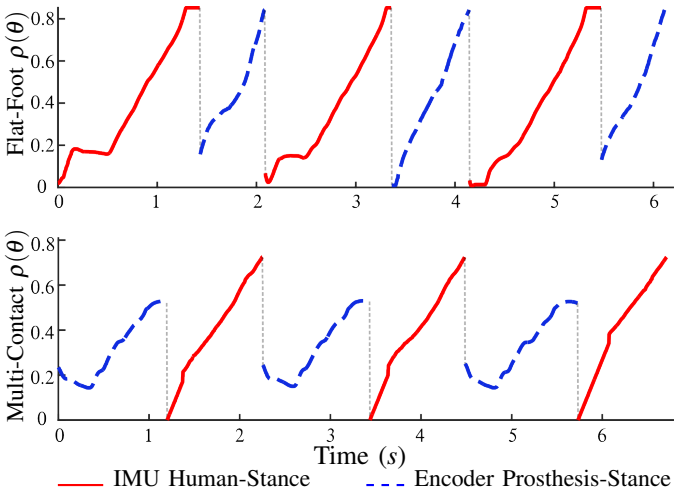


Fig. 8: Phase variable $\rho(\theta)$ comparisons between Experimental flat-foot and multi-contact prosthetic walking over 6 steps. The red solid lines represent $\rho(\theta)$ computed by the IMUs during human-stance phase. The blue dash lines represent $\rho(\theta)$ computed by the encoders during prosthesis-stance phase. $x$-axis is the real-time each step takes.

### A. *Specification of AMPRO*

AMPRO was designed to be a high powered, compact and structurally safe device. The device uses a roller chain drive train consisting of a brushless DC motor and a harmonic gearhead to actuate the ankle and knee joints in the sagittal plane. This design utilizes two incremental encoders for each motor and is designed to incorporate absolute encoders at both actuated joints. Two Elmo motion controllers are used to drive the motors and read the encoder values. Additionally, two FlexiForce force sensors are mounted at the toe and heel to measure the normal reaction forces which are used for the purpose of leg switch. More details about the design specifications can be found in [43].

### B. *Methods*

The architecture of the control scheme for the transfemoral prosthesis includes three hierarchical levels, the pseudo-code of which can be seen in Fig. 6. In particular, a low-level controller is realized in a closed-loop by the ELMO motion drive, which is able to compensate for friction, damping effects and transmission dynamics of the motors. The mid-level controllers generate the input torques for the joints using various controllers. The high-level controller is in charge of the interaction between the robot and human, which includes switching to different domains based on specific criteria and computing the desired trajectories for the domain.

**Desired Trajectory Computing.** As discussed in Sec. III, the outputs are synchronized by the phase variable (4), by knowing which the desired trajectory can be computed using the PHZD reconstruction strategy [16], [23], [41]. During the prosthetic-stance phase, the phase variable and the corresponding hip velocity can be obtained from the encoders directly. To provide a point of human-robotic interaction during the human-stance phase, two IMUs are mounted on the shin and thigh of the human leg to sense the human movement, i.e., the relative orientation and velocity between body segments. The obtained knee and ankle angles/velocities are utilized directly for computing the phase variable. Therefore, prosthetic leg can sense the movement of the human body, and the desired swing trajectories of the prosthesis can be calculated accordingly.

The instrumentation of the human leg with IMUs are not necessary for achieving stable prosthetic walking with the framework in this work. Instead of having a state-base prosthetic swing phase, a time-base swing phase can be implemented without the requirement of the IMUs, which is also a common practice for prosthetic control as discussed in [24], [32]. However, one of main benefits with using the IMUs is that the prosthetic leg is able to react to the human body directly. For example, the prosthetic leg can stop if the human stops during walking while the prosthetic leg is in the swing phase. More importantly, with the augmentation of the IMUs, the amputee can start, stop and change the walking cadence easily and smoothly without requiring any extra effort, which, can benefit the prosthetic walking greatly.

**Domain Switching.** For the multi-contact walking with multiple domains, different sets of outputs are considered for each domain (as discussed in Sec. III). Therefore, the desired trajectory needs to be calculated according to the current domain [41]. During the prosthetic-stance phase, the domain switch can be achieved using the two force sensors mounted on the heel and toe of the prosthetic foot. However, because the human foot is not instrumented, the domain switch is estimated using the phase variable. In particular, the specific phase variable $\rho(\theta)$, at which moment the domain switches, is recorded during the gait design optimization. These values are then utilized as the thresholds to determine the domain switch during human-stance phase in the experiment.

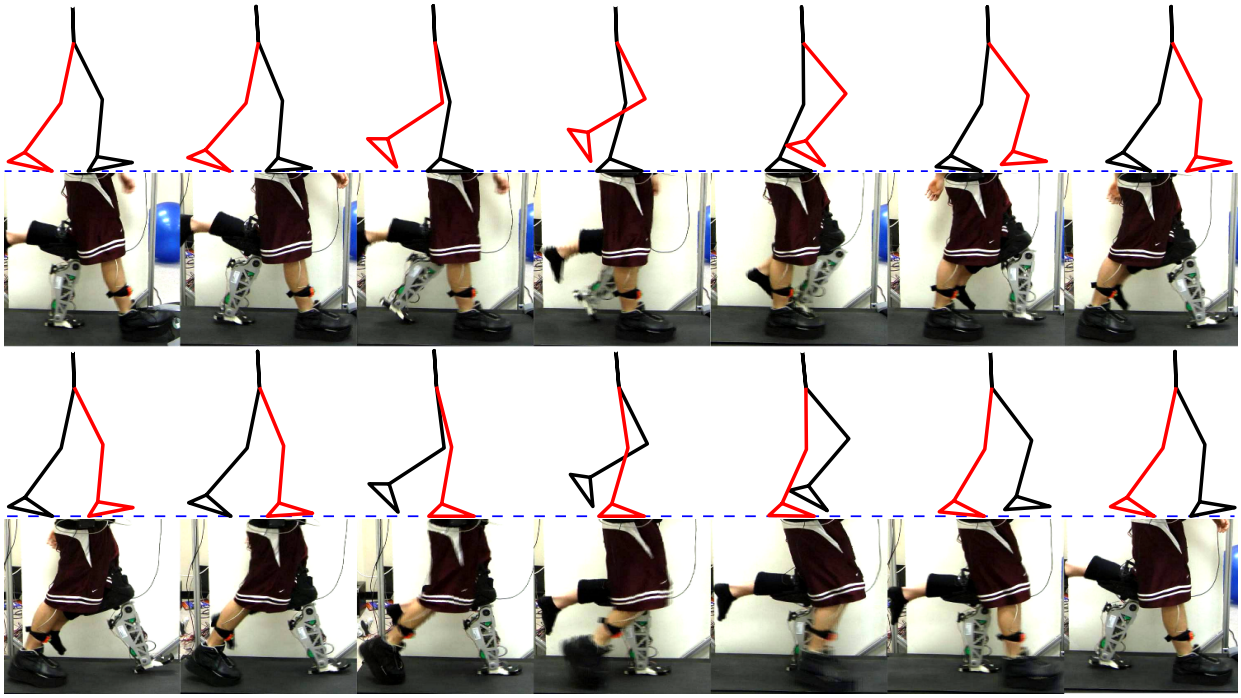

Fig. 9: Gait tile comparisons between the simulated and the experimental prosthetic walking using MIQP+Imp control.

### C. Experiment Results

A PD controller $u^{pd}$ is first implemented to achieve stable walking. Walking trials were performed on a treadmill providing a constant speed of 1.3 mph. The impedance parameters are estimated with the least-square-error fitting method based on the experimental walking data obtained using the PD controller. With the impedance parameters in hand, we apply impedance control $u^{imp}$ as the feed-forward term while using the MIQP control $u^{qp}$ as the feedback term to track the desired joint trajectories. The resulting joint trajectories (averaged over 10 steps) are compared with the designed gait (generated in Sec. III) in Fig. 7, showing that the obtained prosthetic walking is able to realize the designed gait successfully and shares a similar pattern as the healthy human locomotion. The experimental multi-contact phase variable $\rho(\theta)$ is plotted in Fig. 8 with the comparison to the flat-foot walking. The experiment gait tiles of the multi-contact level-ground walking using the proposed optimization-based controller along with the simulated prosthetic walking are shown in Fig. 9. A video of the resulting multi-contact walking can be seen at [2].

For the purpose of control performance comparison, an augmented control strategy, PD+Impedance (i.e., $u_d = u^{pd} + u^{imp}$) is tested in the experiment. Note that, as mentioned in Sec. IV, the torque bounds can be considered inside the quadratic program, therefore yielding the resulted controller (pointwise) optimally satisfying the torque bounds. In particular, two rounds of test with different torque bounds—100 Nm for high torque bounds (MIQPH+Imp) and 40 Nm for low torque bounds (MIQPL+Imp)—are tested to verify the torque optimality. The tracking *rms* errors along with the average power consumption of one step using different controllers are compared in Fig. 10.

**Remark.** One practical problem during testing is that the subject walking with prosthetic devices will not have the same step posture every step, i.e., each step will be slightly different. Also, asymmetry in the gait in the form of short stepping on one leg can cause variations in the starting $\rho(\theta)$. Therefore, the phase variables $\rho(\theta)$ computed from the IMUs and encoders will not evolve exactly as predefined—from 0 to $\rho_{max}(\theta)$ (which is obtained based on the chosen gait). During the human-stance phase, non-zero initial $\rho(\theta)$ will cause problems with yielding a non-smooth prosthetic-swing trajectory, i.e., there will be jumps of the desired position and velocity at the transition from prosthetic-stance to prosthetic-swing. To overcome this problem in the testing, a time-based $\rho(\theta)$ was used at the beginning of the prosthetic-swing phase, in which way the $\rho(\theta)$ will always start from zero to guarantee the smooth transition. Then the $\rho(\theta)$ will switch to state-based when the state-based value is very close (within 0.02 difference) to the time-based value. During the prosthetic-stance phase, due to a flatter pattern of the trajectory (i.e., both the movement ranges and velocities of both the knee and angle joints are small), the non-zero initial $\rho(\theta)$ was not found to be a problem that affects the overall performance during the prosthetic-stance phase.

### D. Discussion

**Comparison of Different Controllers.** The tracking results plotted in Fig. 10 show that the tracking performances of both the ankle and knee are best with MIQPH+Imp control. In particular, we found that with improved tracking performance (12.9% improvement), the MIQPL+Impedance has similar energy consumption (less than 1% difference) when compared with PD control. Similarly, the MIQPH+Impedance outperforms PD+Impedance control in tracking performance

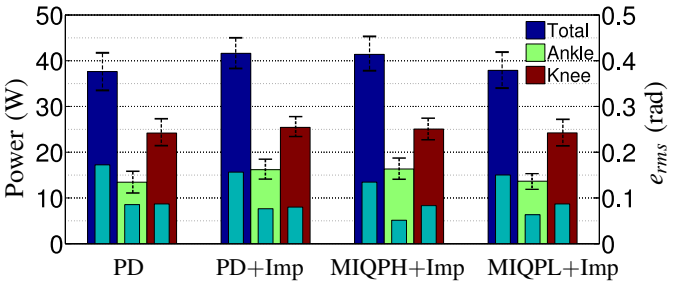


Fig. 10: Net power with one standard deviation (thick bar) and *rms* tracking error (thin bar) comparisons of the prosthetic joints of one step (including stance phase and swing phase) with using different control methods as averaged over 10 steps.

(13.9% improvement) while requiring similar power (less than 1% difference). Note that, traditional control approaches (e.g. variable impedance control) to powered prostheses rely on the extensive tuning of control parameters in order to achieve successful operation of the device for a particular subject. Alternatively, we take the position tracking path with the goal of automating both gait generation and controller design for different subjects and various locomotion types. We believe that a well designed gait (w.r.t power, torque, velocity etc) is the first step toward benefiting the amputee when clinical expertise is also considered in future work. More importantly, this process can be done iteratively in an automatic way such that the performance (e.g., comfortability) can be improved with the feedback from the test subjects. Considering the fact that the proposed control method is based on position tracking, the tracking performance is one of the key aspects for performance comparison. Therefore, to summarize, we can conclude that the MIQP+Impedance controller has a more balanced performance between tracking and power requirements.

**Comparison With Flat-Foot Walking.** In the authors' previous work [43], the proposed optimization-based controller has been utilized to realize flat-foot prosthetic walking. One important improvement can be seen from Fig. 8 by comparing the phase duration symmetry between the multi-contact walking and the flat-foot walking. In particular, during the flat-foot walking, the prosthetic-stance phase duration is $0.65s$, which is much shorter than the $1.33s$ human-stance phase duration (averaged over 5 steps), i.e., the gait is asymmetric w.r.t the phase duration. On the other hand, for the multi-contact walking, the averaged (over 5 steps) prosthetic-stance phase duration is very close to the human-stance phase duration with the time being $1.28s$ and $1.02s$, respectively. Therefore, the multi-contact walking has a much better phase duration symmetry performance than the flat-foot walking.

Due to the flat-foot constraint, the prosthetic ankle movement is limited, therefore yielding a less human-like ankle trajectory. In this work, we explicitly compare the resulting multi-contact joint trajectories with the flat-foot walking obtained from [43] along with the collected unimpaired human locomotion data in Fig. 11. From this comparison, we can see that the multi-contact ankle angle has a more human-like curve pattern as the healthy human ankle. Importantly, the knee trajectory also has more human-like features such as a longer swing phase duration and a bigger stance knee bend when compared to the flat-foot knee trajectory.

Additionally, the most important improvement is achieved with the ankle joint kinetically. The human ankle plays an important role in progressing forward smoothly and efficiently during the stance phase [28]. In particular, the ankle stores the elastic energy in mid-stance phase, which will be utilized to propel the body forward and upward during the foot push off phase [9]. The ankle torque comparison shown in Fig. 11 indicates that the ankle joint in multi-contact walking follows a closer pattern of human walking, which is not seen in the flat-foot walking. More importantly, the user also reported a significant foot push off from the prosthetic device to help propel forward, which is lacking during the flat-foot walking.

## VI. CONCLUSIONS

By leveraging a systematic methodology—including hybrid system models and real-time optimization-based controllers—this paper successfully translated the multi-contact behavior that is intrinsic in human locomotion from bipedal walking on AMBER2 to prosthetic walking on the prosthesis AMPRO. The performance of multiple controllers—utilized to track the generated multi-contact gait—are compared with the real-time optimization-based controller resulting in the best overall performance. The obtained prosthetic walking is shown to capture the essentials of human walking both kinematically and kinetically. This results in a smoother, more symmetric gait duration and more comfortable user experience when compared to flat-foot walking.

## REFERENCES

[1] Multi-Contact Robotic Walking of AMBER. https://youtu.be/VvkIdCKlL54.
[2] Realization of Multi-Contact Prosthetic Walking with AMPRO. https://youtu.be/K6mKYrVYVwE.
[3] M. Ackermann. *Dynamics and Energetics of Walking with Prostheses*. PhD thesis, University of Stuttgart, Stuttgart, March 2007.
[4] N. Aghasadeghi, H. Zhao, L. J. Hargrove, A. D. Ames, E. J. Perreault, and T. Bretl. Learning impedance controller parameters for lower-limb prostheses. *IEEE: IROS*, pages 4268–4274, 2013.
[5] A. D. Ames. Human-inspired control of bipedal walking robots. *Automatic Control, IEEE Transactions on*, 59(5):1115–1130, 2014.
[6] A. D. Ames, E. A. Cousineau, and M. J.Powell. Dynamically stable bipedal robotic walking with nao via human-inspired hybrid zero dynamics. In *Hybrid Systems: Computation and Control*, pages 135–144, Beijing, China, 2012.
[7] A. D. Ames, K. Galloway, K. Sreenath, and J. W. Grizzle. Rapidly exponentially stabilizing control lyapunov functions and hybrid zero dynamics. *Automatic Control, IEEE Transactions on*, 59(4):876–891, 2014.
[8] A. D. Ames, R. Vasudevan, and R. Bajcsy. Human-data based cost of bipedal robotic walking. In *Hybrid Systems: Computation and Control*, pages 153–162, Chicago, IL, 2011.
[9] S. K. Au, P. Dilworth, and H. Herr. An ankle-foot emulation system for the study of human walking biomechanics. In *Robotics and Automation, IEEE International Conference on*, pages 2939–2945, Orlando, 2006.
[10] G. Bessonnet, P. Seguin, and P. Sardain. A parametric optimization approach to walking pattern synthesis. *Int. J. Rob. Res.*, 24(7):523–536, July 2005.
[11] J.A. Blaya and H. Herr. Adaptive control of a variable-impedance ankle-foot orthosis to assist drop-foot gait. *Neural Systems and Rehabilitation Engineering, IEEE Transactions on*, 12(1):24–31, 2004.
[12] C. Chevallereau, D. Djoudi, and J. W. Grizzle. Stable bipedal walking with foot rotation through direct regulation of the zero moment point. *Robotics, IEEE Transactions on*, 24(2):390–401, April 2008.

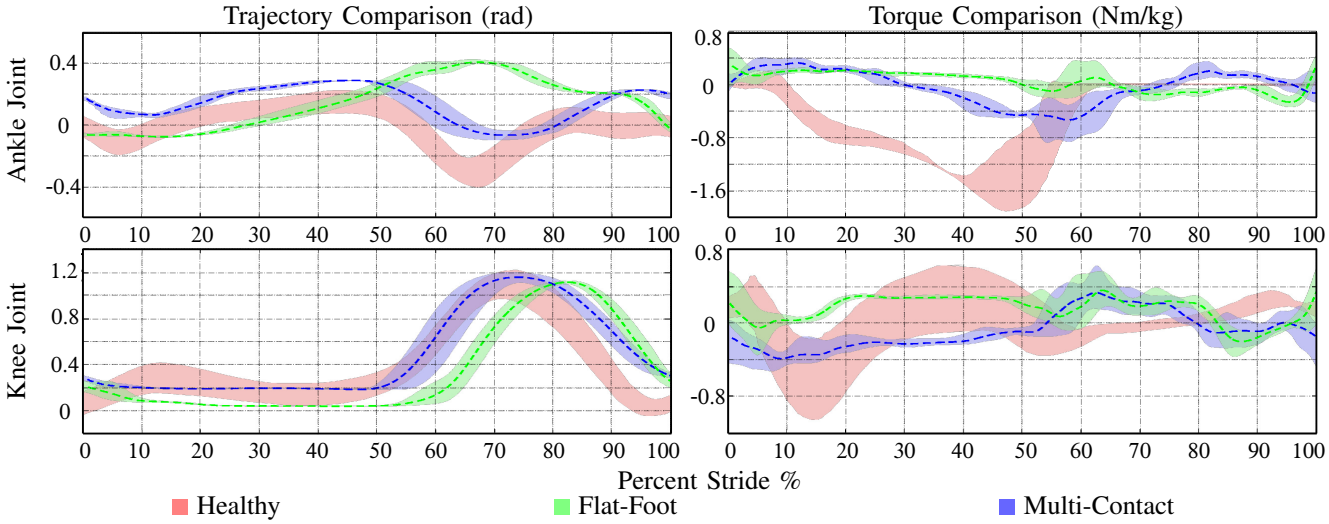


Fig. 11: Comparisons of the joint angles and torques of the healthy human walking (obtained from [37]), the experiment flat-foot and multi-contact prosthetic walking. The shade area is the one standard deviation of corresponding data.


[13] J. W. Grizzle, C. Chevallereau, R. W. Sinnet, and A. D. Ames. Models, feedback control, and open problems of 3d bipedal robotic walking. *Automatica*, 50(8):1955 – 1988, 2014.

[14] J. Weber H. Herr and S. Au. Powered ankle-foot prosthesis. *Biomechanics of the Lower Limb in Health, Disease and Rehabilitation*, pages pp.72–74, 2007.

[15] N. Handharu, J. Yoon, and G. Kim. Gait pattern generation with knee stretch motion for biped robot using toe and heel joints. In *Humanoid Robots, 8th IEEE-RAS International Conference on*, pages 265–270. IEEE, 2008.

[16] A. Hereid, S. Kolathaya, M. S. Jones, J. Van Why, J. W. Hurst, and A. D. Ames. Dynamic multi-domain bipedal walking with atrias through slip based human-inspired control. In *17th International Conference on Hybrid Systems: Computation and Control*, pages 263–272. ACM, 2014.

[17] N. Hogan. Impedance control: An approach to manipulation. pages 304–313, 1984.

[18] K.W. Hollander and T.G. Sugar. A robust control concept for robotic ankle gait assistance. In *Rehabilitation Robotics, ICORR, IEEE 10th International Conference on*, pages 119–123, 2007.

[19] Q. Huang, K. Yokoi, S. Kajita, K. Kaneko, H. Arai, N. Koyachi, and K. Tanie. Planning walking patterns for a biped robot. *IEEE Transactions on Robotics and Automation*, 17:280–289, 2001.

[20] Y. Hürmüzlü and D. B. Marghitu. Rigid body collions of planar kinematic chains with multiple contact points. *Intl. J. of Robotics Research*, 13(1):82–92, February 1994.

[21] V. T. Inman and J. Hanson. Human locomotion. In *Human Walking*. Williams & Wilkins, Baltimore, 1994.

[22] S. Jiang, S. Partrick, H. Zhao, and A. D. Ames. Outputs of human walking for bipedal robotic controller design. In *American Control Conference (ACC)*, pages 4843–4848, June 2012.

[23] J. Lack, M. J. Powell, and A. D. Ames. Planar multi-contact bipedal walking using hybrid zero dynamics. In *Robotics and Automation (ICRA), 2014 IEEE International Conference on*, pages 2582–2588.

[24] E. C. Martinez-Villalpando. Design of an agonist-antagonist active knee prosthesis. *BioRob*, pages 529–534, 2008.

[25] D. C. Morgenroth, A. D. Segal, K. E. Zelik, J. M. Czerniecki, G. K. Klute, P. G. Adamczyk, M. S. Orendurff, M. E. Hahn, S. H. Collins, and A. D. Kuo. The effect of prosthetic foot push-off on mechanical loading associated with knee osteoarthritis in lower extremity amputees. *Gait & posture*, 34(4):502–507, 2011.

[26] B. Morris and J. W. Grizzle. A restricted poincaré map for determining exponentially stable periodic orbits in systems with impulse effects: Application to bipedal robots. In *Decision and Control and European Control Conference. 44th IEEE Conference on*, pages 4199–4206, 2005.

[27] R. M. Murray, Z. Li, and S. S. Sastry. *A Mathematical Introduction to Robotic Manipulation*. CRC Press, Boca Raton, March 1994.

[28] R. R. Neptune, S. A. Kautz, and F. E. Zajac. Contributions of the individual ankle plantar flexors to support, forward progression and swing initiation during walking. *J. of Biomechanics*, 34(11):1387–1398, November 2001.

[29] T. S. Parker and L. O. Chua. *Practical numerical algorithms for chaotic systems*. Springer New York, 1989.

[30] S. S. Sastry. *Nonlinear Systems: Analysis, Stability and Control*. Springer, New York, June 1999.

[31] S. Šlajpah, R. Kamnik, and M. Munih. Kinematics based sensory fusion for wearable motion assessment in human walking. *Computer methods and programs in biomedicine*, 2013.

[32] F. Sup, A. Bohara, and M. Goldfarb. Design and Control of a Powered Transfemoral Prosthesis. *The International journal of robotics research*, 27(2):263–273, February 2008.

[33] D. H. Sutherland, K. R. Kaufman, and J. R. Moitoza. *Human Walking*. Williams & Wilkins, Baltimore, 1994.

[34] D. Tlalolini, C. Chevallereau, and Y. Aoustin. Comparison of different gaits with rotation of the feet for a planar biped. *Robotics and Autonomous Systems*, 57(4):371 – 383, 2009.

[35] E. R. Westervelt, J. W. Grizzle, C. Chevallereau, J. H. Choi, and B. Morris. *Feedback Control of Dynamic Bipedal Robot Locomotion*. CRC Press, Boca Raton, June 2007.

[36] E. R. Westervelt, J. W. Grizzle, and D. E. Koditschek. Hybrid zero dynamics of planar biped walkers. *Automatic Control, IEEE Transactions on*, 48(1):42–56, Jan 2003.

[37] D. A. Winter. *Biomechanics and Motor Control of Human Movement*. Wiley-Interscience, New York, 2 edition, May 1990.

[38] H. Zhao and A. D. Ames. Quadratic program based control of fully-actuated transfemoral prosthesis for flat-ground and up-slope locomotion. In *American Control Conference*, pages 4101–4107, June 2014.

[39] H. Zhao, J. Horn, J. Reher, V. Paredes, and A. D. Ames. A hybrid systems and optimization-based control approach to realizing multi-contact locomotion on transfemoral prostheses. In *Decision and Control (CDC), 2015 IEEE 54nd Annual Conference on*.

[40] H. Zhao, S. Kolathaya, and A. D. Ames. Quadratic programming and impedance control for transfemoral prosthesis. *Robotic and Automation, 2014 IEEE, International Conference on*, pages 1341 – 1347.

[41] H. Zhao, W.-L Ma, M. B. Zeagler, and A. D. Ames. Human-inspired multi-contact locomotion with amber2. In *Cyber-Physical Systems (ICCPS), International Conference on*, pages 199–210, April 2014.

[42] H. Zhao, M. J. Powell, and A. D. Ames. Human-inspired motion primitives and transitions for bipedal robotic locomotion in diverse terrain. *Optimal Control Applications and Methods*, 35(6):730–755, 2014.

[43] H. Zhao, J. Reher, J. Horn, V. Paredes, and A. D. Ames. Realization of nonlinear real-time optimization based controllers on self-contained transfemoral prosthesis. In *6th International Conference on Cyber Physics System*, pages 130–138, Seattle, WA, 2015.

[44] H. Zhao, J. Reher, J. Horn, V. Paredes, and A. D. Ames. Realization of stair ascent and motion transitions on prostheses utilizing optimization-based control and intent recognition. In *Rehabilitation Robotics (ICORR), 2015 IEEE International Conference on*, pages 265–270, Aug 2015.

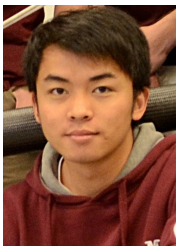

**Huihua Zhao** is currently a Ph.D. student at Georgia Institute of Technology. His research interests focus on formally realizing natural human-like, multi-contact bipedal robotic walking with special emphasis on translating optimal nonlinear robotic control to achieve stable transfemoral prosthetic walking. He received his B.S. in Mechanical Engineering from the University of Science and Technology of China in 2010, and M.S. degree in Mechanical Engineering from Texas A&M University in 2015.

**Jonathan Horn** received the B.S. degree in mechanical engineering from Texas A&M University, College Station, Texas, in 2013. He is currently a Graduate Research Assistant in the department of mechanical engineering at Texas A&M University. His current research interests include the design and control of advanced lower extremity prostheses with a particular focus on anthropomorphically-inspired control of hybrid systems.

**Jacob Reher** received a degree in Mechanical Engineering from the University of Nebraska - Lincoln and is pursuing a Ph.D. at Georgia Institute of Technology. He is currently a Graduate Research Assistant in the department of mechanical engineering at Georgia Institute of Technology. His research interests include the implementation of nonlinear sensing and control algorithms for assistive robotics and bipedal locomotion.

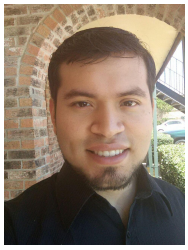

**Victor Paredes** received the B.S degree in Mechatronics Engineering from the National University of Engineering, Peru, in 2012. In 2013 he held a Visiting Scholar status in Texas A&M, College Station, TX. where has pursued a M.S. in Mechanical Engineering since 2014. He is currently a Research Assistant at the Department of Mechanical Engineering at Texas A&M, College Station, TX. His research interests include assistive devices with emphasis on lower-limb prostheses, bipedal walking, robotics and control systems.

**Aaron D. Ames** is an Associate Professor at the Georgia Institute of Technology in the Woodruff School of Mechanical Engineering and the School of Electrical and Computer Engineering. Prior to joining Georgia Tech, he was an Associate Professor and Morris E. Foster Faculty Fellow II at Texas A&M University. Dr. Ames received a B.S. in Mechanical Engineering and a B.A. in Mathematics from the University of St. Thomas in 2001, and he received a M.A. in Mathematics and a Ph.D. in Electrical Engineering and Computer Sciences from UC Berkeley in 2006. He served as a Postdoctoral Scholar in Control and Dynamical Systems at the California Institute of Technology from 2006 to 2008. At UC Berkeley, he was the recipient of the 2005 Leon O. Chua Award for achievement in nonlinear science and the 2006 Bernard Friedman Memorial Prize in Applied Mathematics. Dr. Ames received the NSF CAREER award in 2010 for his research on bipedal robotic walking and its applications to prosthetic devices, and is the recipient of the 2015 Donald P. Eckman Award recognizing an outstanding young engineer in the field of automatic control. His lab designs, builds and tests novel bipedal robots, humanoids and prostheses with the goal of achieving human-like bipedal robotic walking and translating these capabilities to robotic assistive devices.